AERODYNAMIC DERIVATIVES FACTORING SCHEME FOR THE MSC/NASTRAN DOUBLET LATTICE PROGRAM

by

Emil Suciu*, John Glaser** and Rosemary Coll***

Boeing of Canada Ltd.
de Havilland Division

ABSTRACT

A factoring scheme based on correcting a full set of subsonic strip aerodynamic derivatives calculated with the MSC/NASTRAN Doublet Lattice Method is presented. Verification of the procedure was performed by comparing the calculated flutter speeds with existing experimental flutter speeds for an unswept wing with control surface at low speed. The generalized aerodynamic forces are calculated using factored and unfactored aerodynamic derivatives.

---

* Technical Specialist, Structural Dynamics Group
** Chief, Structural Dynamics and Acoustics
*** Supervisor, Engineering Computing Services

LIST OF SYMBOLS

C_p = pressure coefficient.

ΔC_p = $C_{p\ upper} - C_{p\ lower}$.

c = chord.

$\bar{c}$ = reference chord or length.

DLM = Doublet Lattice Method.

h = transverse displacement of lifting surface at reference axis.

i = imaginary unity, also an index.

j = an index.

k = $\frac{\omega c}{2V}$ = reduced frequency, nondimensional. This definition is used in DLM. V = True Airspeed.

k = an index

l = an index.

l = reference length.

$L_h, L_\alpha, L_\beta, L_\delta$ = lift coefficients (derivatives) due to h, α, β, δ motion.

m = an index.

$M_h, M_\alpha, M_\beta, M_\delta$ = moment coefficients (derivatives) about a reference axis due to h, α, β, δ motion.

n = an index.

p = pressure.

q = an index.

$[Q_{hh}]$ = matrix of generalized aerodynamic response forces, NASTRAN notation.

$Q_h, Q_\alpha, Q_\beta, Q_\delta$ = tab hinge moment coefficients (derivatives) due to h, α, β, δ motion.

$T_h, T_\alpha, T_\beta, T_\delta$ = aileron hinge moment coefficients (derivatives) due to h, α, β, δ motion.

x = streamwise coordinate.

z(x) = transverse displacement along strip chord.

w	=	downwash.
α	=	angle of attack.
β	=	aileron rotation angle.
δ	=	tab rotation angle.
ω	=	circular frequency of oscillation.

I. INTRODUCTION

It has long been recognized that calculated two-dimensional unsteady aerodynamic lifts and moments need to be corrected for finite span effects (the original modified strip theory of Yates, Reference 1). In Reference 2, it is pointed out that a complete set of two-dimensional aerodynamic derivatives (lift, moment about a reference axis, control hinge moment and tab hinge moment) need to be corrected for viscosity and thickness effects. General recommendations regarding the magnitude of the factors to be applied to the various derivatives are given in Reference 2. The corrections are based on steady-state experimental measurements.

Three-dimensional lifting surface programs such as the Doublet Lattice Method (abbreviated as DLM), Reference 3, while accounting for finite span, do not model thickness and the boundary layer. The unsteady aerodynamic forces calculated with these programs have the same type of inaccuracies arising from neglecting the wing thickness and the boundary layer as the two-dimensional theories.

Occasionally, a flutter incident occurs such as the one encountered during the flight flutter testing of the T-46A airplane (Reference 4) which was not predicted by initial analysis because a strip theory aerodynamics program was used which had only spanwise lift distribution correction. Analyses subsequent to the flutter incident with factored strip theory-calculated aileron aerodynamic derivative for the aileron rotation mode involved in the flutter mechanism succeeded in predicting the flutter speeds encountered by the aircraft. An analysis using DLM aerodynamics with factored pressures for the aileron rotation mode also predicted the flutter incident.

In recognition of the inherent inaccuracies of the unsteady aerodynamic calculations (both two and three-dimensional) for the flutter analyses of wings with control surfaces and tabs, the U.S. Federal Aviation Administration Advisory Circular AC No: 25.629-1 recommends that: "The aerodynamic coefficients of the control surface and tab used in the flutter analysis should be adjusted to match experimental values at zero frequency. Once the analysis has been conducted with the nominal, experimentally adjusted values of hinge moment coefficients, the analysis should be conducted with parametric variations of these coefficients and other parameters subject to variability."

Attempts to correct the DLM-calculated results have previously been made. Giesing, Kalman and Rodden (Reference 5), Zwaan (Reference 6), Pitt & Goodman (Reference 7) and Wieseman (Reference 8) have proposed correction schemes of varying degrees of complexity.

Commercial software which permits such corrections or factoring of the aerodynamic derivatives in the case of flutter analyses using unsteady 3-D lifting surface aerodynamics programs is not readily available. A need for an aerodynamic derivatives factoring capability is therefore identified for commercial programs in wide use, such as the MSC/NASTRAN (Reference 9). A successful attempt to factor a full set of aerodynamic derivatives calculated with the Doublet Lattice Program as implemented in the MSC/NASTRAN Aeroelastic Package is presented here. The major impetus for this work was the fact that the Boeing of Canada Dash-8 Series of airplanes have control surfaces with horn aerodynamic balance and most of the tab types known: spring tabs, trim tabs and geared tabs. In addition, the full-span rudder is of the serially-hinged type. All these lifting surfaces with their control surfaces and tabs need careful unsteady aerodynamics modelling.

II. DETAILS OF THE FACTORING SCHEME.

The factoring scheme described here bears some similarities with the method of Zwaan (Reference 6) and of Pitt and Goodman (Reference 7).

The present factoring scheme is tied with MSC/NASTRAN modal analysis and interpolation of modal motion at the aerodynamic grid points. Throughout this discussion it is assumed that the reader is familiar with the MSC/NASTRAN DLM terminology. It is also assumed that the panelling schemes used in a MSC/NASTRAN DLM analysis yield converged numerical results. It is emphasized that the present factoring method is not intended to be used for improving incorrect results caused by the use of poor panelling techniques.

The discussion which follows applies to each elastic mode considered in a flutter analysis. The elastic motion for any given streamwise strip is assumed to consist of superimposed wing bending, wing torsion, control rotation and tab rotation. See Figure 1. This elastic motion is decomposed or "descrambled" into pure motions: rigid heave, rigid pitch defined about an elastic axis, rigid control rotation and rigid tab rotation. See again Figure 1.

Motion where streamwise cambering deformation occurs is not considered in this discussion. Such motion is now under investigation and results will be presented in a future reference.

The steps described below refer to any chordwise strip on the lifting surface, for any elastic mode.

A post processing program has been written which generates the same aerodynamic box arrangement as the one generated by MSC/NASTRAN DLM and all the calculations described here are performed on this set of boxes. The steps in the calculations are:

1. For each mode, at each chordwise strip, descramble the general elastic motion into rigid heave, rigid pitch, rigid control rotation and rigid tab rotation. The calculation of h, α, β, δ proceeds on the modal displacements outputted by MSC/NASTRAN at the aerodynamic grid points (centers of the boxes). The general elastic motion for any given mode of motion, for any given aerodynamic strip looks like:

$$\begin{bmatrix} z_1 \\ z_2 \\ \vdots \\ z_i \\ z_{i+1} \\ \vdots \\ z_{i+j} \\ \vdots \\ z_{i+k} \\ \vdots \\ z_n \end{bmatrix} = \begin{bmatrix} h \\ h \\ \vdots \\ h \\ h \\ \vdots \\ h \\ \vdots \\ h \\ \vdots \\ h \end{bmatrix} + \begin{bmatrix} \alpha*\Delta x\alpha_1 \\ \alpha*\Delta x\alpha_2 \\ \vdots \\ \alpha*\Delta x\alpha_i \\ \alpha*\Delta x\alpha_{i+1} \\ \vdots \\ \alpha*\Delta x\alpha_{i+j} \\ \vdots \\ \alpha*\Delta x\alpha_{i+k} \\ \vdots \\ \alpha*\Delta x\alpha_n \end{bmatrix} + \begin{bmatrix} 0. \\ 0. \\ 0. \\ 0. \\ 0. \\ 0. \\ \vdots \\ \beta*\Delta x\beta_1 \\ \vdots \\ \beta*\Delta x\beta_q \\ \vdots \\ \beta*\Delta x\beta_s \end{bmatrix} + \begin{bmatrix} 0. \\ 0. \\ \vdots \\ 0. \\ 0. \\ \vdots \\ 0. \\ \vdots \\ \delta*\Delta x\delta_1 \\ \vdots \\ \delta*\Delta x\delta_m \end{bmatrix}$$

where

$\Delta x\alpha$ is measured from the reference axis to the aerodynamic grid point

$\Delta x\beta$ is measured from the control hinge line to the aerodynamic grid point

$\Delta x\delta$ is measured from the tab hinge line to the aerodynamic grid point.

2. MSC/NASTRAN DLM requires the downwash to be calculated at the 3/4 chord of each aerodynamic box. The motions calculated at Step 1 are at

1/2 box chord. They will be extrapolated linearly to the 3/4 box chord location.

3. The downwash is calculated based on the descrambled motions at Step 1. Instead of a single downwash vector, we now have 4 downwash vectors, which add up to the original one as a check.

4. From MSC/NASTRAN Solution Sequence 75 the inverse of the aerodynamic influence coefficient matrix, $[A]^{-1}$ is obtained. This matrix is multiplied with the four descrambled downwash vectors calculated at Step 3 and for each elastic mode, a set of 4 descrambled pressure vectors, each due strictly to h, α, β and δ motions, respectively, is obtained:

$$\{\Delta Cp\}_i = [A]^{-1} * \{w\}_i \quad \text{or} \quad \begin{bmatrix} \Delta Cph_1 & \Delta Cp\alpha_1 & \Delta Cp\beta_1 & \Delta Cp\delta_1 \\ \vdots & \vdots & \vdots & \vdots \\ \Delta Cph_n & \Delta Cp\alpha_n & \Delta Cp\beta_n & \Delta Cp\delta_n \end{bmatrix}$$

where n is the number of aerodynamic boxes.

5. For each aerodynamic strip, integrate the 4 descrambled pressures for each mode to obtain the strip lift due to h, α, β and δ motions, moment about the reference axis due to h, α, β and δ, control hinge moment due to h, α, β and δ motions and tab hinge moment due to h, α, β and δ.

6. The matrix of correction factors necessary to factor the strip quantities calculated at Step 5 looks like:

$$\begin{bmatrix} fL_h & fL_\alpha & fL_\beta & fL_\delta \\ fM_h & fM_\alpha & fM_\beta & fM_\delta \\ fT_h & fT_\alpha & fT_\beta & fT_\delta \\ fQ_h & fQ_\alpha & fQ_\beta & fQ_\delta \end{bmatrix}$$

These correction factors are based on steady-state experimental data. If no experimental data or established guidelines are available for some correction factors, they should be left equal to 1. If the wing lift has been factored, the moment about the reference axis should be factored by the same number as the lift.

The correction of the strip lift, moment, control hinge moment and tab hinge moment is:

$$L' = L_h * fL_h + L_\alpha * fL_\alpha + L_\beta * fL_\beta + L_\delta * fL_\delta$$

$$M' = M_h * fM_h + M_\alpha * fM_\alpha + M_\beta * fM_\beta + M_\delta * fM_\delta$$

$$T' = T_h * fT_h + T_\alpha * fT_\alpha + T_\beta * fT_\beta + T_\delta * fT_\delta$$

$$Q' = Q_h * fQ_h + Q_\alpha * fQ_\alpha + Q_\beta * fQ_\beta + Q_\delta * fQ_\delta$$

The primed quantities L', M', T' and Q' are the factored strip lift, moment, control hinge moment and tab hinge moment.

7. The generalized aerodynamic response airforces matrix with corrected strip derivatives is:

$$[Q_{hh}] = \begin{matrix} \text{NMODE} \\ \text{NMODE} \end{matrix} \begin{bmatrix} \text{NSTRIP} \\ h',\alpha',\beta',\delta' \ \ldots \ h',\alpha',\beta',\delta' \\ \vdots \\ h',\alpha',\beta',\delta' \ \ldots \ h',\alpha',\beta',\delta' \end{bmatrix} \times \begin{matrix} \text{NMODE} \\ \text{NSTRIP} \end{matrix} \begin{bmatrix} L' \ldots L' \\ M' \ldots M' \\ T' \ldots T' \\ Q' \ldots Q' \\ \vdots \\ L' \ldots L' \\ M' \ldots M' \\ T' \ldots T' \\ Q' \ldots Q' \end{bmatrix}$$

8. If a change in the location of the center of pressure is desired for any given strip, the moment about the reference axis will have to change also. This change is additive. By requiring a change in Δxc_p, the change in moment is calculated:

$$\Delta M_\alpha = L_\alpha * \Delta xc_p$$
$$\Delta M_\beta = L_\beta * \Delta xc_p$$
$$\Delta M_\delta = L_\delta * \Delta xc_p$$

Note that if the matrix of correction factors contains only unit factors, the generalized forces matrix calculated at Step 7 is identical with the one calculated by MSC/NASTRAN DLM operating on the scrambled motions.

III. NUMERICAL RESULTS.

The calculations described in the previous section have been incorporated into a computer program. As described, the calculation of the downwash, the calculation of the descrambled pressure vectors, the factoring of the strip derivatives and the calculation of the generalized aerodynamic forces take place outside MSC/NASTRAN. These factored generalized forces are inserted back into the MSC/NASTRAN flutter solution sequence through the use of DMAP ALTERs. See Figure 2 for a schematic of the modified flutter solution sequence.

Results have been obtained for a rectangular wing of AR=8 with aileron extending over the outer 50% of the semi-span (wing 5 with aileron AII of Reference 10). See Figure 3 for the planform and mass properties of this wing-aileron combination (as a reminder, motion descrambling for this type of wing is exact). The stiffness properties of this wing are known, as are the springs which define the aileron frequencies. The first wing bending frequency is 10.68 Hz. The first wing torsional frequency is above 50 Hz and therefore the torsional degree of freedom will not be used in the analysis. See Table I for a summary of the vibration characteristics of this wing-aileron combination.

Two degrees of freedom are used in the present analysis. The first one is the first wing cantilevered bending. The additional degree of freedom is the aileron rotation.

MSC/NASTRAN results are superimposed over the original NACA results in Figure 4. An uncorrected MSC/NASTRAN strip theory flutter solution was performed first, with good agreement with the experimental data, showing a degree of conservatism. The original unfactored MSC/NASTRAN DLM-calculated flutter speeds are also plotted in this Figure. The wing-aileron planform as used in the strip theory analysis and the doublet lattice aerodynamic analysis is also shown in Figure 4. Note the difference in predicted flutter speeds between MSC/NASTRAN calculations with strip aerodynamics and unfactored DLM aerodynamics.

The strip theory derivatives are incorrect, since they are purely two-dimensional. The DLM-calculated derivatives, while likely also incorrect, are nevertheless believed to be closer to reality than the 2-D ones, yet their inclusion into the generalized forces produces incorrect flutter speeds. No experimental derivatives data is available for wing 5 with aileron AII. Attempts to factor the DLM aerodynamic derivatives have been undertaken in the form of parametric

variations in the active derivatives for this problem, which are L_h, L_β, T_h and T_β, following the guidelines set in Reference 2. It is quickly established that variations of the control surface hinge moment derivative due to bending, T_h, do not affect the calculated results significantly, so T_h will be factored by 1.0 from now on. The other three derivatives do affect these calculations, and the following results show this. Figure 5 shows the same results as Figure 4, but the flutter speeds predicted with factored DLM derivatives (L_h*1.0, L_β*0.75, T_β*0.6) are also included. There is a noticeable improvement in the predicted higher speed flutter boundary, but flutter is still not predicted for aileron rotation to wing bending frequency ratios above 1.1.

It is recognized that a significant degree of freedom contributing to the aerodynamic damping and stiffness is the bending degree of freedom. Results with factored L_h are shown in Figure 6 (L_h*0.6, L_β*1.0, T_β*0.9). Note that flutter is predicted beyond the aileron rotation/wing bending frequency ratio of 1.1, but flutter at zero speed with damping very close to zero occurs at frequency ratios of aileron rotation/wing bending below 0.6. Bergh and Tijdeman (Reference 11) have found that calculated flutter at zero speed is possible in certain cases of two-degree-of-freedom, two dimensional conditions with factored derivatives, so that this result is not outlandish. Note also that the reduced frequency is rather large at the low speed flutter boundary.

A better knowledge of derivatives will likely bring the calculated flutter speeds in better agreement with the experimental values.

Another example of the use of the factoring scheme described here is in the analytical treatment of single-side failures of control surfaces or tabs. This problem is non-symmetrical in nature, but as will be shown shortly, a half model in conjunction with factoring of the pertinent aerodynamic derivatives can reliably be used to simulate such failures. Wing 5 with Aileron AII of NACA Report No 685 provides the ideal test problem. The left-hand-side of this wing-aileron combination was modelled and the complete wing, capable of simulating nonsymmetrical behaviour was analyzed free-free. Figure 7 shows the aerodynamic panelling of the complete wing-aileron combination. The active degrees of freedom for this problem are the wing first few vertical bending modes (both symmetric and antisymmetric) and the aileron rotation modes, also symmetric and antisymmetric. The aileron failure or aileron disconnected condition is simulated by having an aileron rotational frequency of about 0.2 Hz. Two rigid-body modes are present, heave and roll about the wing centerline. For the following sequence of runs, the aerodynamic derivatives are factored either by 1.0 or by 0.5, as indicated in the context. Figure 8 shows the V-g-f plot for the nonsymmetrical wing with both ailerons disconnected. The aileron symmetric and antisymmetric rotational frequencies are almost identical, at about 0.2 Hz. The first

wing vertical bending frequency is at slightly above 16 Hz, and it is a symmetric mode. The first wing antisymmetric bending mode is at slightly above 46 Hz. The flutter mechanism in this Figure involves the symmetric aileron rotation mode with the symmetric wing bending mode. The predicted onset of flutter is at about 90 mph. The wing antisymmetric bending mode does not interact with either aileron to result in a flutter mechanism. Figures 9 and 10 show the symmetric and antisymmetric free-free flutter analyses using only half of the wing model. Note that a superposition of Figures 9 and 10 would recreate Figure 8.

Figure 11 shows the V-g-f plot for the complete wing, but with the port aileron locked and the starboard aileron failed, thus rendering the problem nonsymmetrical. It is apparent that the flutter mechanism involves the starboard aileron rotation mode and the wing first symmetrical bending mode. The flutter speed is higher, at about 110 mph, and the mechanism is milder than when a double failure occurs, as seen from Figure 8. Based on the observation that the wing symmetrical bending mode is involved in the flutter mechanism, a run is made with a "symmetrized" wing-aileron: the wing properties are the same, but the failure is assumed to involve a port and starboard aileron, each having half mass and inertia as well as forcing the aileron-related aerodynamic derivatives to be 1/2 the original values. Figure 12 shows the V-g-f plots for this idealization of the problem. The flutter speed and general character of the flutter solution are very similar, but not quite identical with the ones shown in Figure 11. Figure 13 shows the V-g-f plots for the symmetric free-free half wing with half aileron weights, inertias and aerodynamic derivatives and Figure 14 shows the corresponding antisymmetric ones. As before, note that the symmetric and antisymmetric free-free solutions of Figures 13 and 14, if superimposed, would recreate the solution for the nonsymmetrical wing-aileron problem seen in Figure 12. This leads one to surmise that an accurate analysis of a single side control surface or tab failure can be done using a "symmetrized halved" model.

IV. CONCLUSIONS.

A method to factor a full set of aerodynamic derivatives calculated by the Doublet Lattice program in its MSC/NASTRAN implementation has been developed and results have been presented which show that manipulation of these derivatives is possible. In the results presented, factoring of the derivatives results in an improvement in predicted flutter speeds. A useful application of the factoring scheme for treating single side control surface or tab failures using a half airplane model is presented.

V. REFERENCES

1. Yates, E. C. Jr., "Calculation of Flutter Characteristics for Finite Span Swept or Unswept Wings at Subsonic and Supersonic Speeds by a Modified Strip Analysis", NACA RM L57L10 (1958).

2. Guyett, P.R., "Empirical Values of Derivatives", AGARD Manual on Aeroelasticity, Part II, Vol. II, March 1961.

3. Giesing, J.P., Kalman, T.P., and Rodden, W.P., "Subsonic Unsteady Aerodynamics for General Configurations", AFFDL-TR-71-5, Part II, Vol. I, Air Force Flight Dynamics Laboratory, Air Force Systems Command, Wright-Patterson Air Force Base, Ohio, November, 1971.

4. French, M., Noll, T., Cooley, D., Moore, R., and Zapata, F., "Flutter Prediction Involving Trailing-Edge Control Surfaces", J. Aircraft, Vol. 25, No. 5, May 1988, pp 393-394.

5. Giesing, J.P., Kalman, T.P., and Rodden, W.P., "Correction Factor Techniques for Improving Aerodynamic Prediction Methods", NASA CR-144967, NASA Langley Research Center, May 1976.

6. Zwaan, R.J., "Verification of Calculation Methods for Unsteady Airloads in the Prediction of Transonic Flutter", Journal of Aircraft, Vol. 22, No. 10, October 1985, pp 833-839.

7. Pitt, D.M., and Goodman, C.E., "Flutter Calculations Using Doublet Lattice Aerodynamics Modified by the Full Potential Equations", AIAA Paper No. 87-0882 presented at the AIAA 25th Aerospace Sciences Meeting, Reno, Nevada, January 1987.

8. Wieseman, C.D., "Methodology for Matching Experimental and Analytical Aerodynamic Data", Paper No. 88-2392, 29th Structures, Structural Dynamics and Materials Conference, Williamsburg, Virginia, April 18-20, 1988.

9. "MSC/NASTRAN Version 64 User's Manuals, Vols I & II, MSC/NASTRAN Aeroelastic Supplement", The MacNeal-Schwendler Corporation, Los Angeles, California, U.S.A..

10. Theodorsen, T., and Garrick, I.E., "Mechanism of Flutter: A Theoretical and Experimental Investigation of the Flutter Problem", NACA Report No. 685, Washington, D.C., 1940.

11. Bergh, H., and Tijdeman, H., "Binary Wing-Control Surface Flutter Calculations with Theoretical and Empirical Aerodynamic Derivatives for Two-Dimensional Incompressible Flow", NLR TR 68069 U, National Aerospace Laboratory, The Netherlands, 1968.

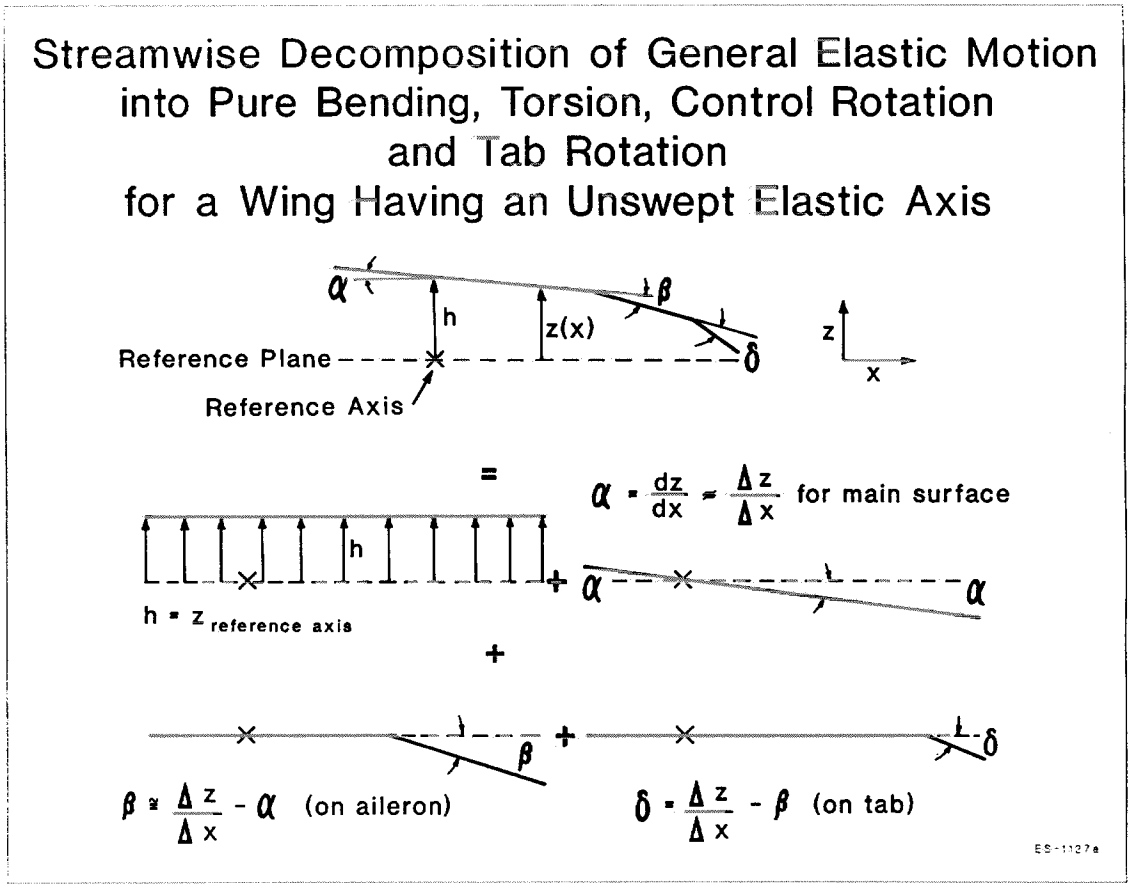

Figure 1

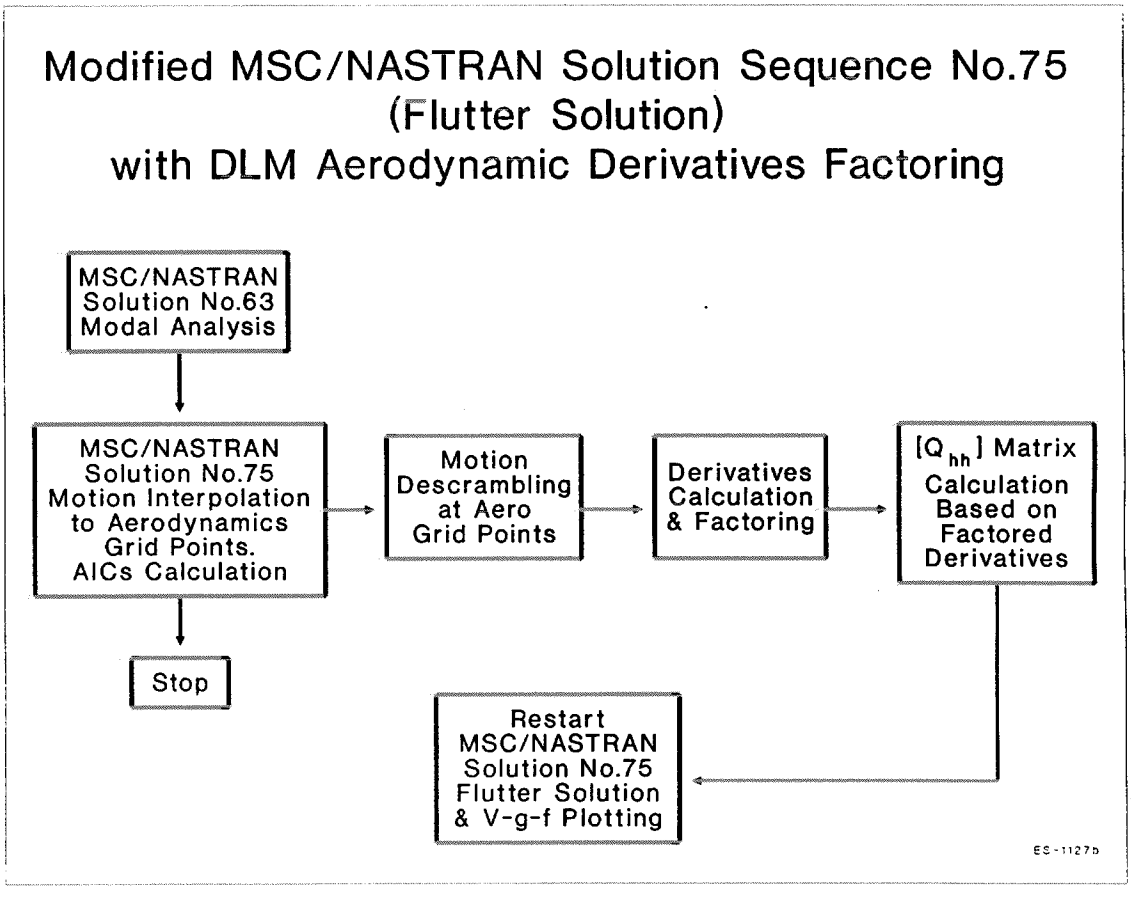

Figure 2

Geometry and Mass Properties for Wing 5 with Aileron All of NACA Report No.685 (Reference 10)

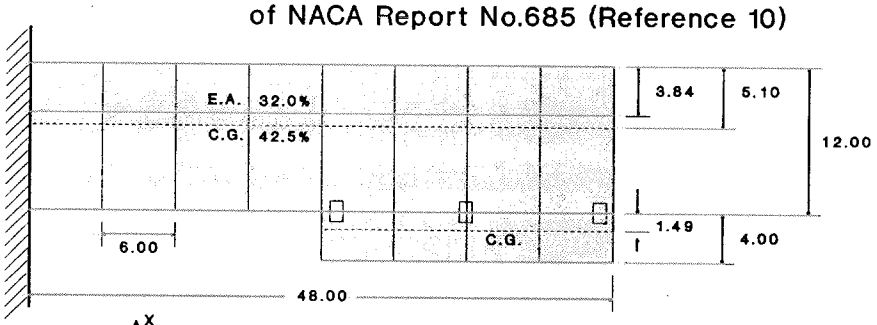

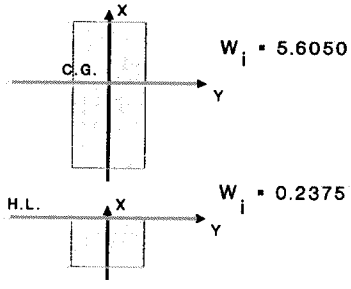

- Wing weight = 44.84 (for the half shown).
- Constant cross-section.
- For each wing strip: $r_{xx} = \sqrt{\frac{I_{xx}}{W}} = 2.00$
- Wing torsional degrees of freedom not considered.
- For each aileron strip:

  $r_{xx} = 2.00$

  $r_{yy} = 1.72955$ about the hinge line

E.A. -- Elastic Axis, at 32% of the chord
C.G. -- Centre of Gravity of wing section, at 42.5% of the chord
H.L. -- aileron Hinge Line, at wing trailing edge

- All dimensions are in inches.
- All weights are in pounds.

ES-1207a

Figure 3

Uncoupled and Coupled Wing and Aileron Frequencies for Wing 5 and Aileron All

Uncoupled Wing Bending Frequency is ω_h = 10.68 Hz

Uncoupled Aileron Frequency ω_β, Hz	Coupled Aileron Frequency ω_β, Hz	Coupled Wing Frequency ω_h, Hz	Uncoupled Frequency Ratio ω_β / ω_h	Coupled Frequency Ratio ω_β / ω_h
0.22	0.22	10.61	0.020	0.020
5.75	5.72	10.67	0.538	0.536
8.50	8.31	10.85	0.796	0.766
11.00	11.78	9.91	1.030	1.188
12.50	13.00	10.20	1.170	1.274
13.10	13.56	10.26	1.226	1.322

ES-1208a

Table 1

Comparison between NACA Report No.685
Experimental and Theoretical Flutter Speeds
with MSC/NASTRAN Calculations for Wing 5 with Aileron All

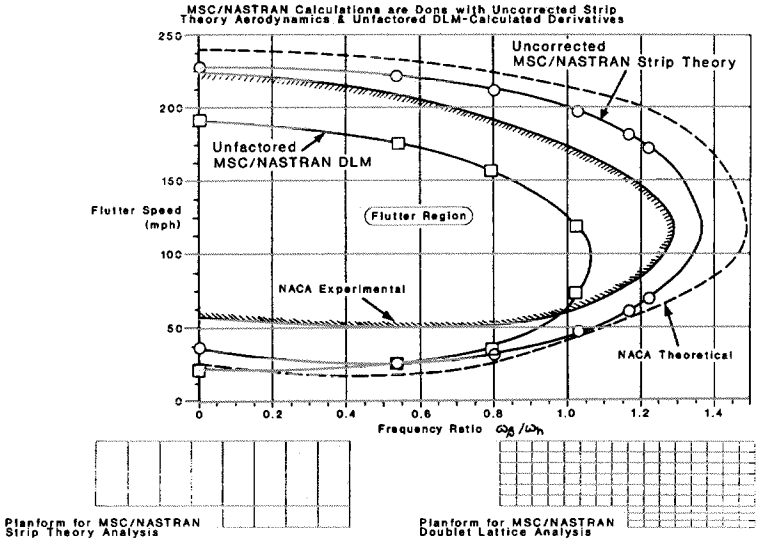

Figure 4

Comparison between NACA Report No.685
Experimental and Theoretical Flutter Speeds
with MSC/NASTRAN Calculations for Wing 5 with Aileron All

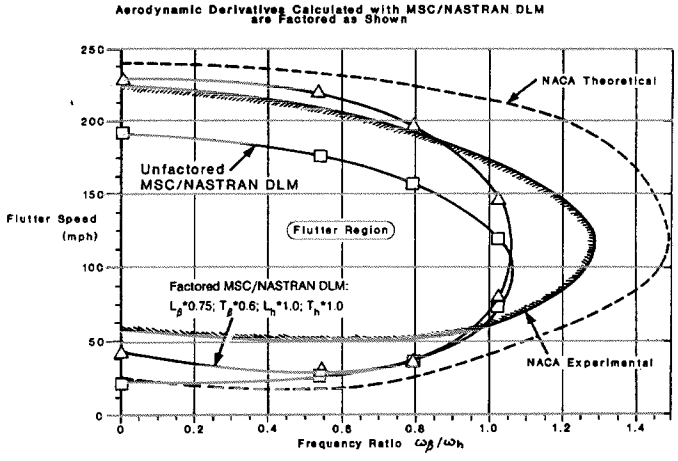

Figure 5

Comparison between NACA Report No.685
Experimental and Theoretical Flutter Speeds
with MSC/NASTRAN Calculations for Wing 5 with Aileron All

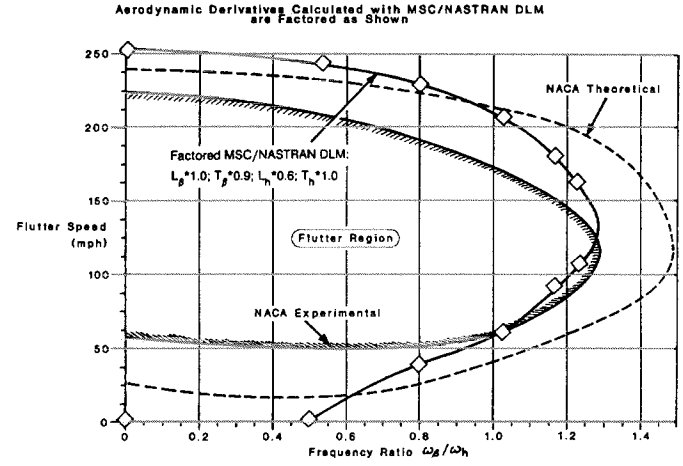

Figure 6

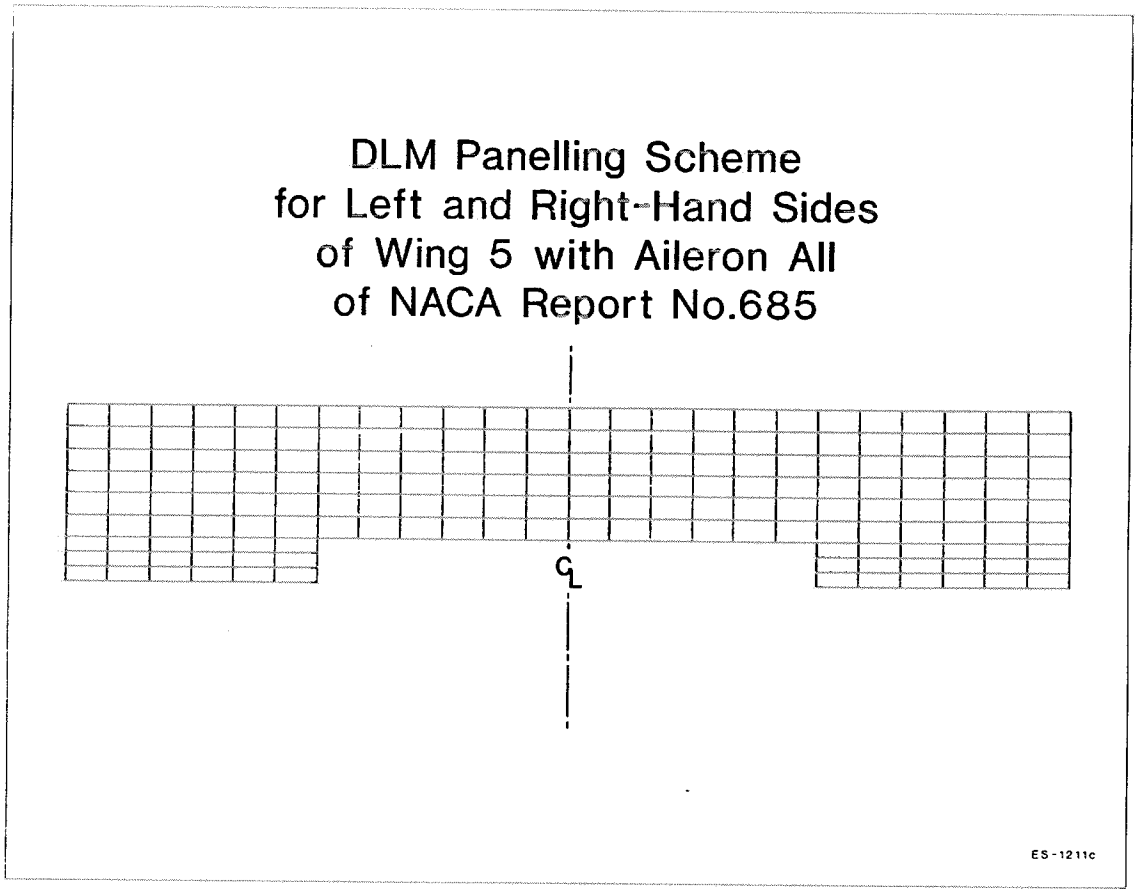

Figure 7

V-g-f Plots for NACA Report No.685

Wing 5 with Aileron All Analyzed Free-Free, Non-Symmetrically

- Both Sides of the Wing and both Ailerons are Present
- Ailerons-Disconnect Condition is Simulated
- P-K Method Flutter
- No Aerodynamic Derivatives Factoring

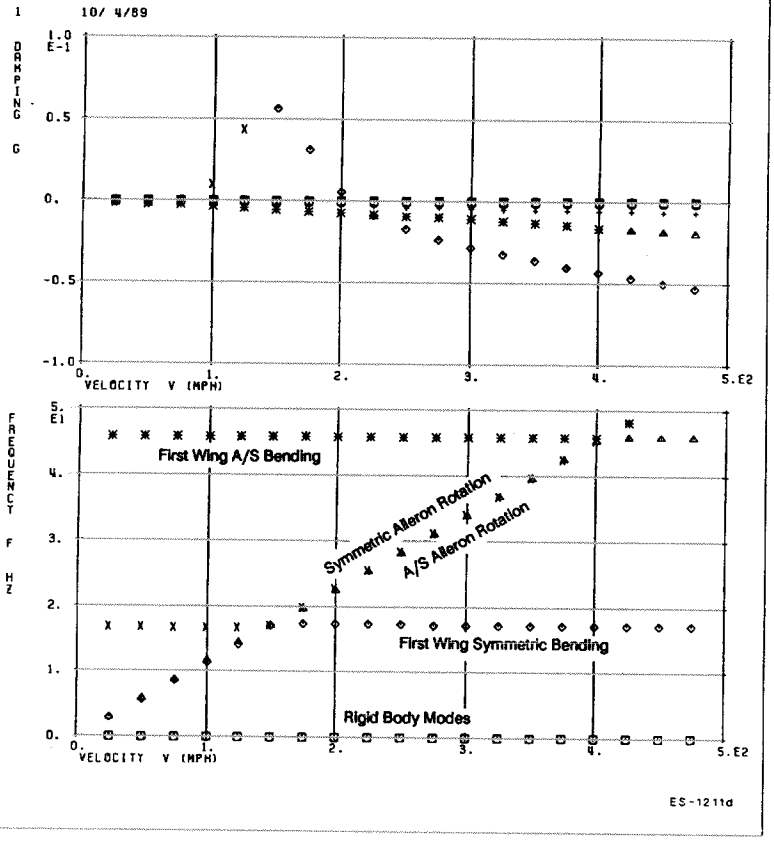

Figure 8

Free-Free
Symmetric Analysis
of
Half Wing-Aileron
Model

- No Derivatives Factoring
- P-K Method Flutter

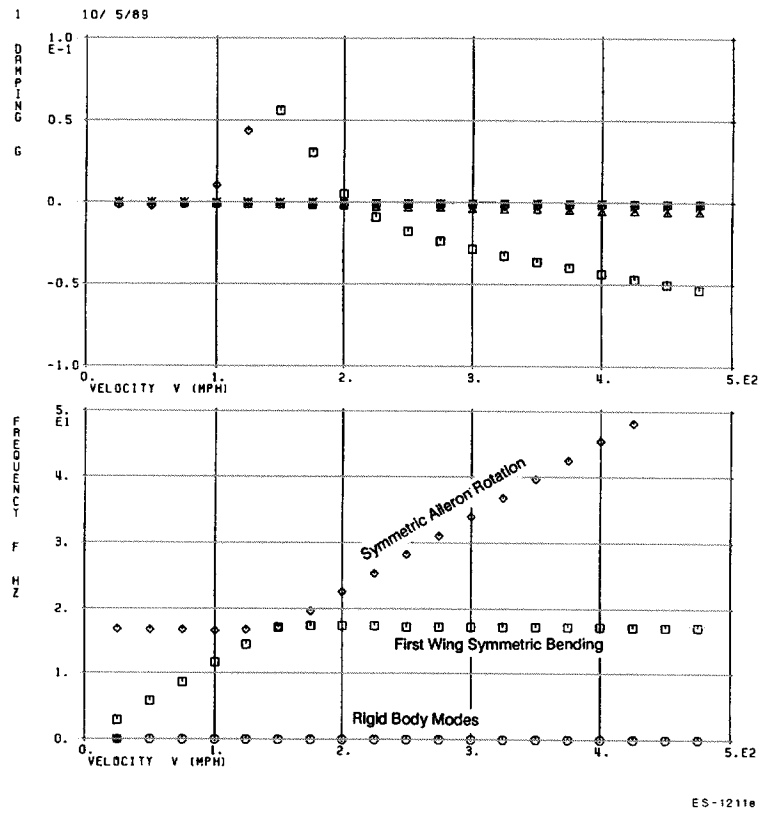

Figure 9

Free-Free
Anti-Symmetric Analysis
of
Half Wing-Aileron
Model

- No Derivatives Factoring
- P-K Method Flutter

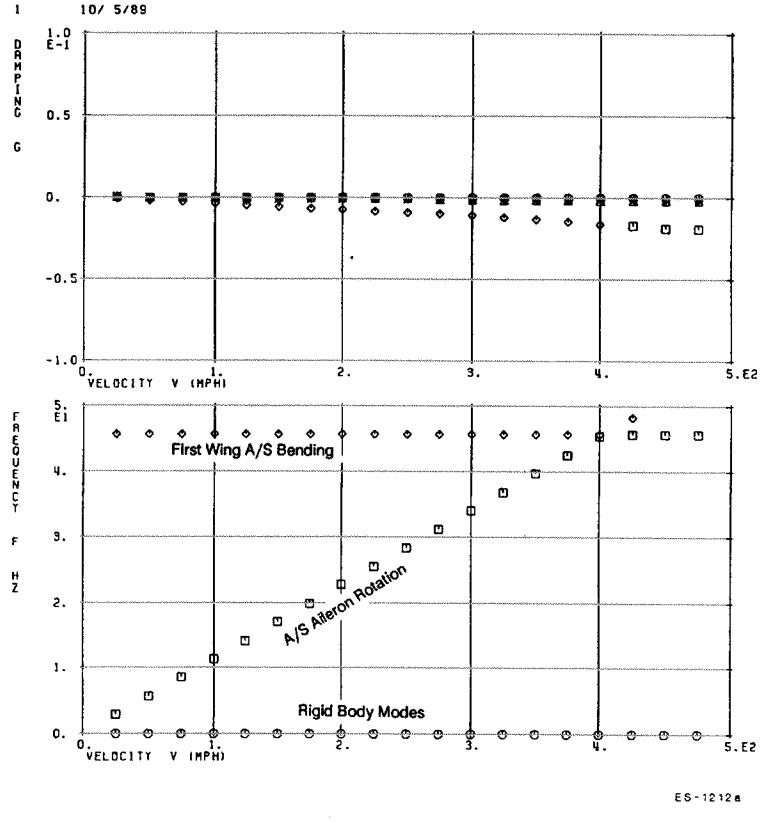

Figure 10

Free-Free
Non-Symmetric Analysis
of
Full Wing-Aileron
Model

- Port Aileron is Locked
- No Derivatives Factoring
- P-K Method Flutter

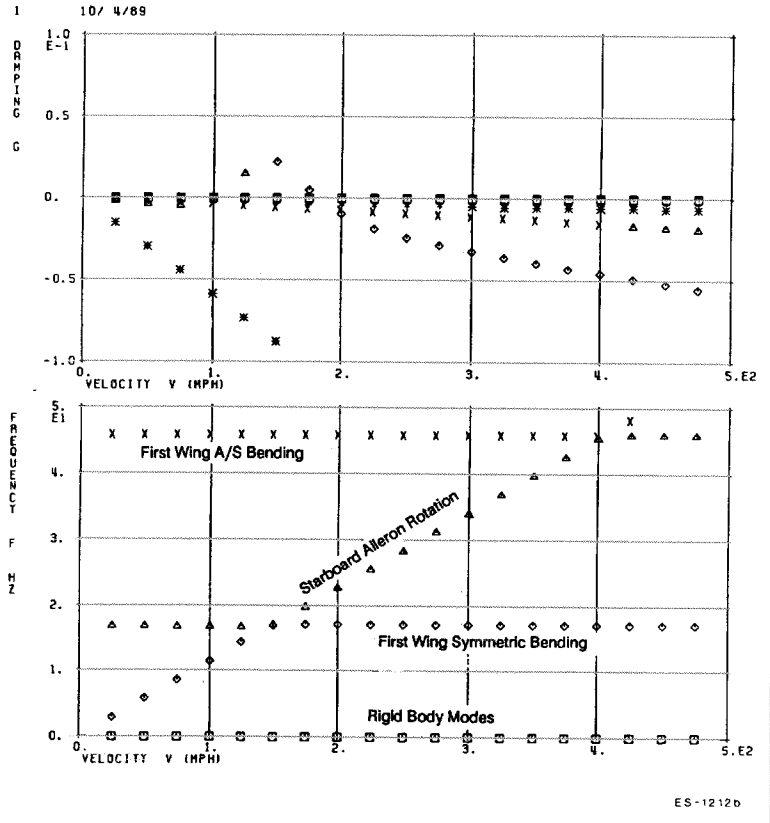

Figure 11

Free-Free
Non-Symmetric
Analysis of
Full Wing-Aileron
Model

- Both Ailerons are Disconnected
- Both Ailerons have Half their Original Weight and Inertia Properties
- Aileron-Related Aerodynamic Derivatives are Factored by 0.5
- P-K Method Flutter

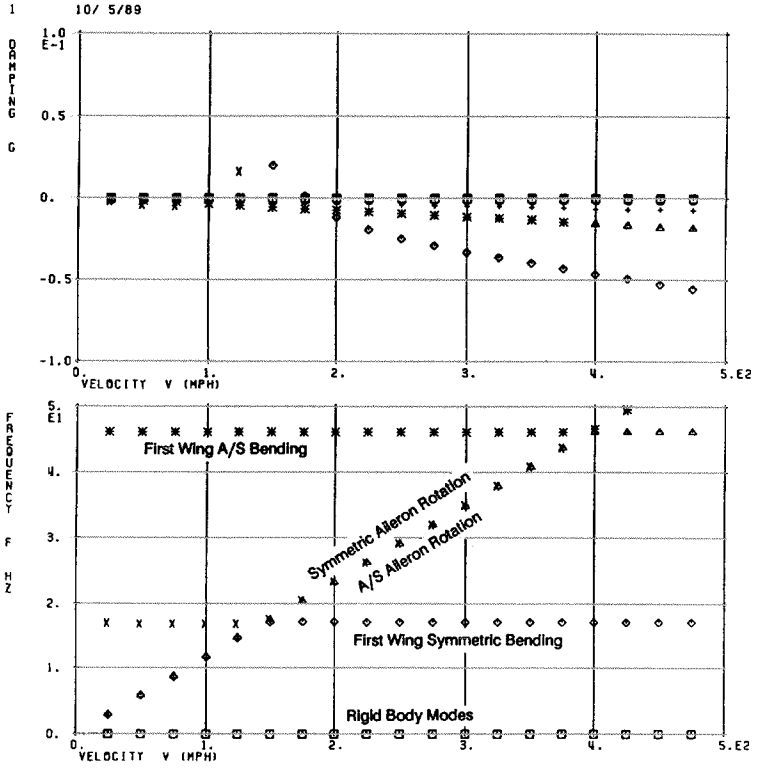

Figure 12

Free-Free Symmetric Analysis of Half Wing-Aileron Model

- Aileron is Disconnected, with Half the Original Weight and Inertia Properties
- Aileron-Related Aerodynamic Derivatives are Factored by 0.5
- P-K Method Flutter

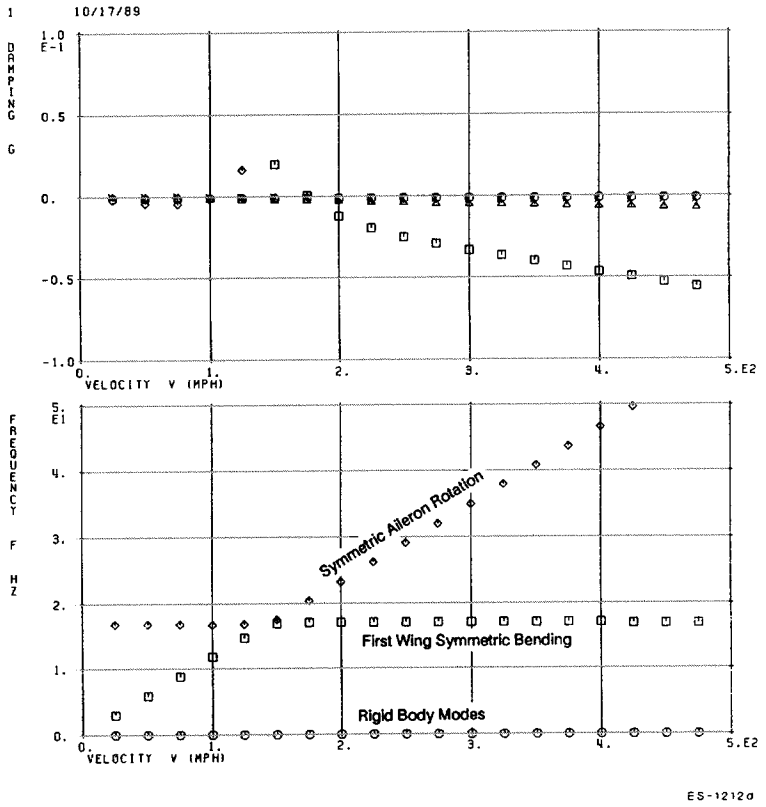

Figure 13

Free-Free Anti-Symmetric Analysis of Half Wing-Aileron Model

- Aileron is Disconnected, with Half the Original Weight and Inertia Properties
- Aileron-Related Aerodynamic Derivatives are Factored by 0.5
- P-K Method Flutter

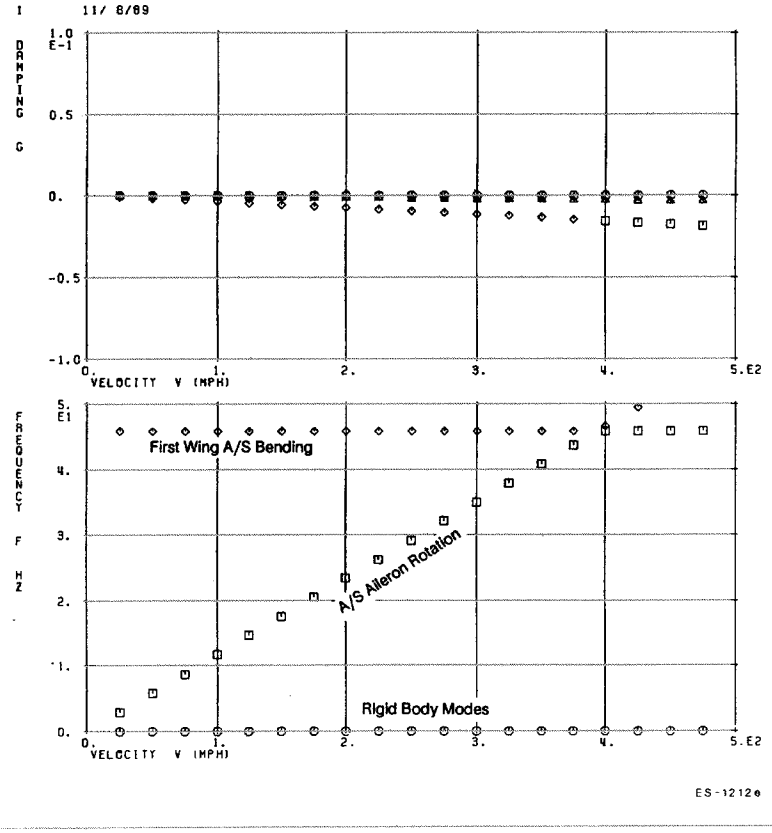

Figure 14